Desalination and Water Treatment
www.deswater.com

doi: 10.5004/dwt.2018.21840

102 (2018) 264–272
January

Removal of disperse dye from aqueous solution in fixed-bed column by water treatment residuals

Mahesh R. Gadekar, M. Mansoor Ahammed*

Civil Engineering Department, S V National Institute of Technology, Surat, 395007, India,
emails: mansoorahammed@gmail.com (M.M. Ahammed), maheshgadekar@ymail.com (M.R. Gadekar)

Received 21 July 2017; Accepted 21 December 2017

ABSTRACT

The present study assessed the potential of aluminium-based water treatment residuals (WTR) for removal of disperse dye, Disperse Navy Blue 3G from aqueous solution. Continuous flow column tests were performed by varying bed depth and flow rate using an influent dye concentration of 100 mg/L. The breakthrough curves were analysed and modelled using Thomas model and bed depth service time (BDST) model and produced good agreement with experimental results. The results showed that both flow rate and bed depth had significant influence on the sorption capacity and breakthrough time, and a maximum uptake capacity of 2.90 mg/g was observed. The study showed that though complete removal of dye cannot be achieved with WTR, it can be used as a primary treatment which would reduce further treatment costs.

Keywords: Adsorption; Disperse dye; Water treatment residuals; Fixed bed column tests; Thomas model; BDST model

1. Introduction

Consumption of large quantity of water in dyeing processes subsequently produces considerable amount of coloured wastewater [1]. Further, dyes are generally non-biodegradable in nature, and their stability towards oxidising agents makes the selection of dye removal methods complex [2,3]. Also, public perception of colour makes great influence on water quality as it is the first contaminant to be recognised in water [4–6]. The presence of colour/dye in water bodies limits light penetration, which in turn disturbs photosynthesis and biological processes in water bodies [5–7]. Stringent governmental legislation and the need to provide an effective process that can efficiently remove these dyes at low cost in a sustainable way have made the wastewater treatment an environmental challenge.

Colour removal can be achieved by either concentrating the colour into sludge or the complete destruction of the dye molecule [8]. Several physicochemical and biological methods have been reported for colour removal such as membrane filtration/separation, coagulation/flocculation, precipitation, flotation, adsorption, ion exchange, ultrasonic mineralisation, electrolysis, chemical reduction, advanced chemical oxidation, and aerobic and anaerobic biological processes [2,4,9–12]. Adsorption process has been investigated due to its simplicity of design, ease of operation and good efficacy. A number of studies on colour removal using different adsorbents such as activated carbons (AC) and bio-waste derived AC have been reported in the literature [5,13–15]. However, preparation and production of AC involves processing of raw material and control of process parameters to obtain quality AC which increases the cost of the treatment process.

Large quantities of sludge are produced in water treatment plants around the world during the removal of fine suspended solids from source water. The water treatment residuals (WTR) are the settled by-product of the coagulation/flocculation which involves addition of aluminium or iron salts. In India, nearly all water treatment plants use aluminium compounds as coagulant [16,17]. The WTR is mainly comprising of metal (aluminium) hydroxide used and destabilised colloids enmeshed within the floc of hydroxide [18–21]. There is a need to manage these residuals in a

* Corresponding author.

sustainable and environmental friendly manner. The waste is generally regarded as non-hazardous and is disposed of as landfills or through land application. In India, however, it is still disposed of into water bodies [18,22].

Adverse environmental effects have been observed in water bodies due to disposal of WTR. Aluminium species toxicity towards various aquatic life and benthic organisms has been reported [23]. This has initiated investigations on potential strategies for WTR utilisation in different wastewater treatment operations. One option is the recovery of aluminium from WTR and its use as coagulant. The other option is the direct reuse of WTR as a coagulant or as an adsorbent. Recovery of aluminium from WTR could be costlier due to process and allied chemicals. However, reusing it directly could be a better option to fully utilise the potential of WTR as a coagulant or sorbent by elimination of the recovery cost. A few studies have been reported on dye removal using Al-based WTR. Chu [20] and Moghaddam et al. [24] reported the use of Al-based WTR for dye removal while Moghaddam et al. [25] studied the use of ferric-based sludge for dye removal. Gadekar and Ahammed [4] reported the use of Al-based wet sludge (WTR) for disperse dye removal by coagulation process. The WTR have also been used as a sorption/filtration medium for removal of phosphorous and heavy metals [19,26–31]. However, no studies have been reported using dry form of WTR as a sorption medium for dye removal. For industrial application, removal of dyes in fixed-bed columns would be more useful compared with the batch systems due to the adaptability of column systems [32].

The present study focused on the potential of aluminium-based water treatment residual as a low-cost sorbent for removal of a disperse dye. Continuous flow fixed-bed sorption study was performed by varying bed depth and flow rate. Breakthrough curves were generated for different operating conditions. The data were modelled using Thomas model. The parameters required for scale-up of the process was determined using bed depth service time (BDST) method.

2. Materials and methods

2.1. Synthetic dye wastewater

A widely used disperse dye in India – Disperse Blue 79 (trade name Disperse Navy Blue 3G) was obtained from Colourtex India Ltd., Surat, India. The CI number, commercial name and chemical structure of the dyestuff are shown in Fig. 1. Stock solution of 1,000 mg/L was prepared dissolving accurate quantity of the dye in distilled water. Synthetic wastewater was prepared by diluting the stock solution with distilled water for desired concentration.

Disperse Blue 79 (Disperse Navy Blue 3G)

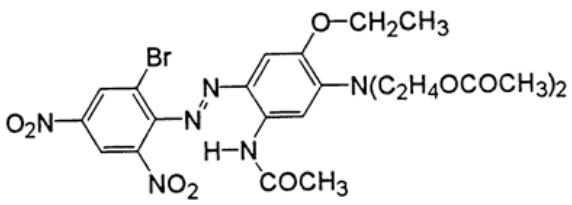

Fig. 1. CI number, commercial name and chemical structure of dyestuff.

2.2. Water treatment residuals

The WTR used in the present study was collected from the coagulation/flocculation unit of a water treatment plant in Bhandup, Mumbai, India, where poly-aluminium chloride (PACl) is used as a coagulant. The sludge collected in wet form was sun dried and ground, and the fraction passed through 216 μm sieve was used as sorbent without further modification.

2.3. Characterisation of WTR

The total metal present in the WTR was determined by acid digestion method of USEPA 3050B [33] and analysed using inductively coupled plasma atomic emission spectroscopy (Element XR, Thermo Fisher Scientific, Germany). Physical and chemical analyses of the WTR surface were carried out by X-ray fluorescence (XRF) using X-ray spectrophotometer (Model-ZSX Mini 2, Rigaku, Japan) and scanning electron microscopy–energy dispersive spectroscopy (SEM–EDS, S-3400, Hitachi, Japan) analysis was performed to understand the surface characteristics. FT-IR spectra of raw and dye-loaded WTR were obtained through FT-IR spectroscopy (8400S, Shimadzu, Japan).

2.4. Point zero charge

The zero point charge (pH_{zpc}) of WTR was evaluated by referring to the procedure of Mehdi et al. [11]. The pH_{zpc} of WTR was determined adopting the following procedure: 0.01 M NaCl solution with different initial pHs in the range of 2–10 were prepared by adding HCl/NaOH. Thereafter, 0.20 g of the WTR was added to 50 mL of 0.01 M NaCl solution of different pHs in reagent bottles. The samples were centrifuged after allowing them to react for 48 h at room temperature and the pH of each solution was measured.

2.5. Fixed-bed column tests

Continuous flow column experiments were conducted in a transparent cylindrical acrylic column (2.5 cm internal diameter and 30 cm height). At the top and bottom of the column, brass converter and nipple were attached to maintain uniform bed height of the sorbent. Glass wool was used to provide support and to avoid the loss of sorbent. A known quantity of WTR was placed in the column to yield the desired bed height of the sorbent. The column was operated in upward mode by pumping the dye solution through the column at a desired flow rate using peristaltic pump. Samples were collected at different time intervals and were analysed for dye removal using a UV–Vis spectrometry (spectrophotometer – 169, Systronics, India) by monitoring the absorbance changes at the wavelength of maximum absorbance (532 nm). Operation of the column was stopped when the effluent dye concentration reached the influent concentration. The dye removal was calculated using the following equation:

$$\text{Colour removal}(\%) = (C_o - C_e)/C_o \times 100 \quad (1)$$

where C_o and C_e are dye concentration of raw and treated solutions, respectively. Effect of two factors were studied, that is, flow rate at 50, 75 and 100 mL/h and bed depth at 5, 10 and 15 cm. In all the tests initial dye concentration was maintained at 100 mg/L with an initial pH 6.90.

2.6. Column data analysis

The performance of fixed-bed columns is presented as breakthrough curves. The time for breakthrough appearance and the shape of the breakthrough curve are very important characteristics for determining the operation and dynamic response of an adsorption column [34,35]. The point where the effluent concentration reaches 95% is usually called the 'point of column exhaustion' [36]. The breakthrough curve is usually expressed by C_e/C_o as a function of time or volume of the effluent for a given bed depth. The volume treated (V) was calculated by flow rate multiplied by exhaustion time. The amount of the total mass of dye removed, q_{total}, was calculated from the area under the breakthrough curve (Eq. (2)).

$$q_{\text{total}} = Q\int_{t=0}^{t=t_{ex}} C\,dt \quad (2)$$

where Q is the volumetric flow rate, t_{ex} is the total flow time, C is the concentration of dye removed. Dye uptake capacity of the column q_{eq} is calculated using Eq. (3):

$$q_{\text{eq}} = \frac{q_{\text{total}}}{m} \quad (3)$$

where m is the dry weight of the sorbent.

2.7. Thomas model

Breakthrough curves or concentration–time profile for the effluent is required for successful design of column sorption process. The Thomas model is generally used for this purpose. The maximum adsorption capacity of an adsorbent is also needed to design a column. The model has the following form [32]:

$$\frac{C_e}{C_o} = \frac{1}{1 + e^{\left(\frac{K_{\text{th}} q_m m}{Q} - K_{\text{th}} C_o t\right)}} \quad (4)$$

where K_{th} is the Thomas rate constant (mL/min mg), and q_m is the maximum solid phase concentration of the solute (mg/g). To calculate the Thomas model constant, Eq. (4) can be linearised as follows (Eq. (5)). The kinetic coefficients K_{th} and q_m for adsorbent bed can be determined from slope and intercept from plot of $\ln(C_o/C_e - 1)$ against time for particular flow rates and bed heights.

$$\ln\left(\frac{C_o}{C_e} - 1\right) = \frac{K_{\text{th}} q_m m}{Q} - K_{\text{th}} C_o t \quad (5)$$

2.8. Bed depth service time method

BDST method is based on the Bohart–Adams equation which can be utilised for the adsorption or filtration column design [37]. The Bohart–Adams equation (Eq. (6)) is based on the fact that breakthrough time is a function of depth of bed, rate of flow and influent concentration:

$$\ln\left(\frac{C_o}{C_e}\right) = K_{\text{ba}} C_o t - K_{\text{ba}} N_o \left(\frac{Z}{u}\right) \quad (6)$$

where K_{ba} is kinetic constant (L/mg h), N_o is the saturation concentration (mg/L), Z is the bed depth (cm) and u is the superficial velocity (cm/min) defined as volumetric flow rate Q (mL/min) to the cross sectional area of adsorbent bed. The modified Bohart–Adams equation can be expressed as follows [32]:

$$t = \frac{S_c Z}{C_o u} - \frac{1}{K_a C_o} \ln\left(\frac{C_o}{C_e} - 1\right). \quad (7)$$

where K_a is the attachment coefficient (L/mg h) which describes attachment of solids to filter media and S_c is the storage capacity (mg/L) which depicts volumetric capacity of adsorbent to store solids [37]. The constants S_c and K_a can be calculated using linear regression analysis between time and bed height.

3. Results and discussion

3.1. Characteristics of water treatment residuals

Figs. 2(a) and (b) depict typical SEM images of the WTR, suggesting concentration of particles around 100 μm size. The amorphous nature of the WTR particles is clearly visible in Fig. 2(b). This is similar to amorphous aluminium hydroxide [38] characterised by the formation of organic ligands [39] formed during the coagulation of water. The energy dispersive X-ray spectrum of WTR (Fig. 2(c)) shows abundance of five elements namely Al, Fe, Mg, Si and Ca. The pH of WTR

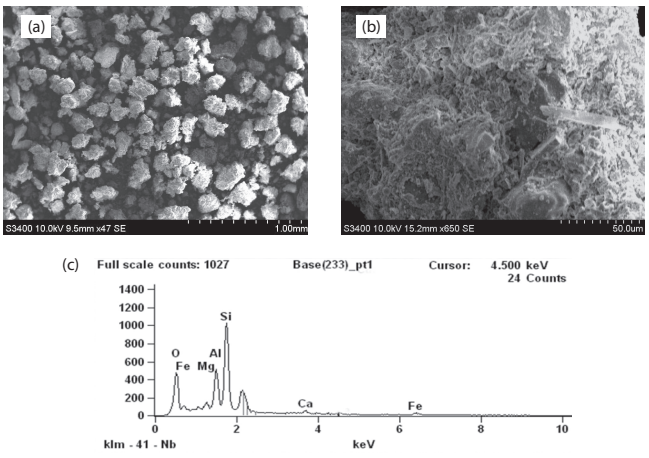

Fig. 2. SEM (a and b) and EDS (c) spectrum of water treatment residuals.

was found to be 6.4. The amount of aluminium and other metals in WTR is presented in Table 1. The results of XRF analysis showed presence of Al_2O_3 (53.45%), Fe_2O_3 (28.73%), CaO (9.50%) and MgO (6.37%), and trace amounts of oxides of S, Cr, Mn, Cu and Zn. Inorganic anions can be adsorbed onto aluminium oxides by ion pair formation with charged surface sites or by ligand exchange with surface hydrolysis [39]. The non-bonding oxygen from these ligands structure may constitute the adsorption availability on WTR surface. As ligand exchange reaction replaces hydroxyls on the surface, the adsorption increases with decrease in pH [39]. The point zero charge (pH_{zpc}) of WTR was estimated to be 6.9 which shows that no significant charge on WTR would be present at neutral pH values. Thus, sorption of cations and anions could be possible by charge neutralisation on to the WTR surface at these pHs.

3.2. Effect of bed height

The breakthrough curves obtained for different bed heights (5, 10 and 15 cm) at a flow rate of 75 mL/h and initial dye concentration of 100 mg/L are presented in Fig. 3.

Table 1
Metal content in water treatment residuals (mg/g of dry sludge)

Parameter	Value
Al	64.60
Fe	93.01
Ca	27.27
Mg	17.34
K	20.06
pH	6.4

The sorption data were evaluated and total amount of dye adsorbed (q_{total}), empty bed contact time (EBCT), exhaustion time (t_{ex}) and volume treated (V) are presented in Table 2. The EBCT was increased from 20 to 60 min with increase in the bed depth from 5 to 15 cm and the corresponding exhaust time was found to have increased from 26.67 to 65.67 h. It can be seen from Table 2 that the bed uptake capacity and breakthrough time increased with increase in the bed height. This increase in the sorption was due to the increase in sorbent mass in the larger beds, which provided more adsorption sites for the dye. Moreover, the gradient of breakthrough curve decreased with increased bed height which resulted in broadening of mass transfer zone and subsequent saturation of adsorbent [40]. Similar trend of decrease of the slope with increase in bed depth has been reported in the literature [41,42]. As presented in Fig. 3, complete colour removal was not observed even at the initial stages of column operation with any of the column height. However, the column showed good removal at C_e/C_o values greater than 0.4. This could be due to increasing formation of non-crystalline aluminium hydroxide and subsequent sorption of dye [39]. The shape of breakthrough curves was 'L(c)' [43] which indicate that adsorption species might have associated into very large clusters before adsorption was taking place. Since complete removal of dye was not obtained even at initial stages, the WTR can be utilised for primary treatment which should be followed by further treatment in order to attain satisfactory dye removals.

3.3. Effect of flow rate

The dispersion characteristics are strongly affected by the changing flow or velocity distribution. The effect of flow rate on dye adsorption was investigated by varying the flow rate from 50 to 100 mL/h. The breakthrough curves for a bed depth

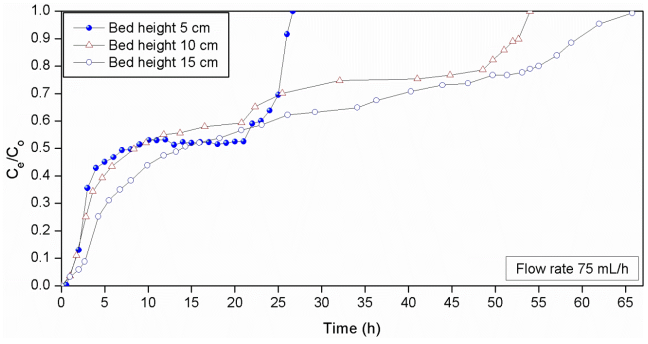

Fig. 3. Breakthrough curves for dye removal at different bed depths (flow rate 75 mL/h).

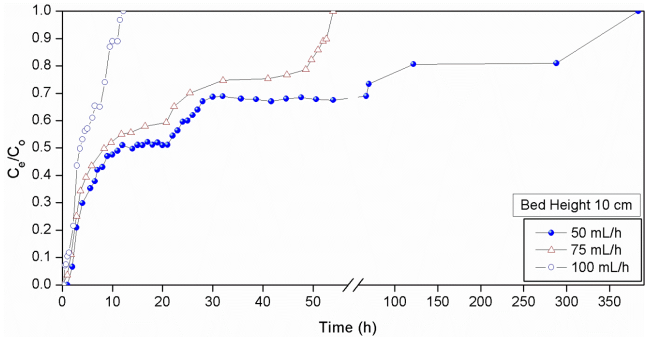

Fig. 4. Breakthrough curve for dye removal at different flow rates (10 cm bed depth).

Table 2
Column data and parameters obtained at different bed depths

S. No.	Bed depth (cm)	Empty bed contact time, EBCT (min)	Total dye adsorbed, q_{total} (mg)	Exhaustion time, t_{ex} (h)	Volume treated, V (L)
1	5	20	91.22	26.67	2.00
2	10	40	134.74	54.00	4.05
3	15	60	171.59	65.75	4.93

Table 3
Column data and parameters obtained at different flow rates

S. No.	Flow rate (mL/h)	Empty bed contact time, EBCT (min)	Total dye adsorbed, q_{total} (mg)	Exhaustion time, t_{ex} (h)	Volume treated, V (L)
1	50	60	341.87	384.00	28.80
2	75	40	134.74	54.00	4.05
3	100	30	107.18	12.17	0.91

of 10 cm at various flow rates are shown in Fig. 4. It can be seen from Fig. 4 that the breakthrough occurred considerably faster with increasing flow rate. As the flow rate was increased from 50 to 100 mL/h, the EBCT decreased from 60 to 30 min and the exhaust time was found to have decreased from 384 to 12.2 h. The breakthrough curves became steeper with increase in flow rate due to reduced contact time. The dye uptake was reduced from 342 to 108 mg as the flow rate was increased from 50 to 100 mL/h (Table 3). The early breakthrough indicates requirement of larger bed depth with adequate contact time. The radial and axial dispersion of adsorbate is controlled by the flow rate. At lower flow rate radial dispersion leads to accumulation of dye through the column which reduced with increase in the flow rate as characterised by shape of breakthrough curve. Effects of axial dispersion are similar as reported in the literature [41]. Thus, increased flow rate reduces the dispersion which in turn decreases the uptake of dye.

3.4. Effect of contact time and flow rate

Fig. 5 shows the effects of EBCT and flow rate on breakthrough time at 40% breakthrough point. The breakthrough time increased with increase in contact time. Longest EBCT was 90 min at 50 mL/h and the breakthrough time obtained was 10.5 h while the shorter EBCT of 15 min was observed for 100 mL/h flow and breakthrough time was observed as 2.2 h. Thus, low flow rate and large bed depth would increase the EBCT of column consequently increasing the breakthrough time of bed column. The larger EBCT may add sufficient radial dispersion in bed with axial dispersion. This could lead to increase in breakthrough time. The slow process of diffusion through or around the sorbent surface material for longer contact time leads to maximum bed volume treatment. Adsorption onto WTR was controlled by both contact time and flow rate as slow process of diffusion through or around surface of material is controlled by contact time.

3.5. Effluent pH

The effluent pH was monitored for various bed depths and the results are shown in Fig. 6. The influent pH was 6.9 while point zero charge (pH_{zpc}) was also found to be 6.9. It can be seen from Fig. 6 that initially pH decreased with the time. With further operation, the effluent pH increased and stabilised at the influent pH values. In WTR depending on solution pH, aluminium may exist in ionic form such as Al^{3+}, $Al(OH)^{2+}$, $Al(OH)_2^+$ or $Al(OH)_4^-$ [39]. The dissolution of Al ions was more at lower pH, thus as aluminium dissolves more H^+ would be hydrolysed.

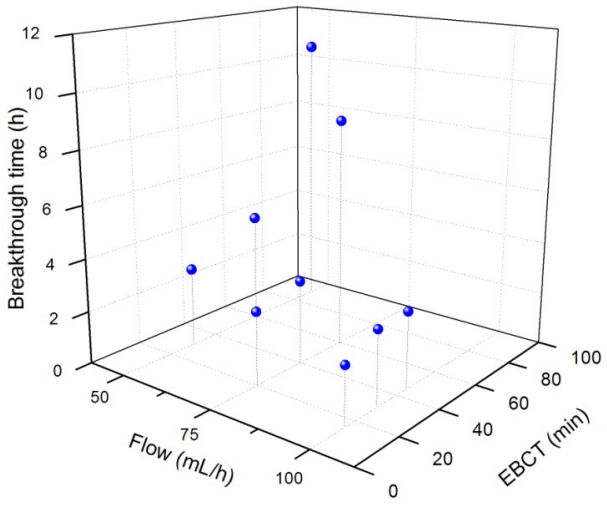

Fig. 5. Effect of flow rate and empty bed contact time (EBCT) on breakthrough time at 40% breakthrough point.

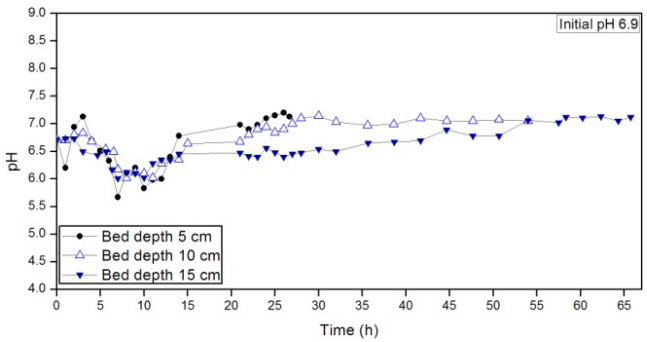

Fig. 6. Variation in effluent pH at various bed depths (flow rate 75 mL/h).

$$Al^{3+} + H_2O \rightleftharpoons Al(OH)^{2+} + H^+ \quad (8)$$

$$Al^{3+} + 2H_2O \rightleftharpoons Al(OH)^{2+} + 2H^+ \quad (9)$$

Thus, initially aluminium present in the WTR was hydrolysed to release H^+ which resulted in the reduction in effluent pH [44]. Moreover, solid phase consumed Al while release of H^+ by means of Al dissolution, preventing further decrease in solution pH. Thus, aluminium dissolution and pH decline are mutually influential on sorption of dye onto WTR. Alumina has shown good adsorption ability for anions at lower pH than pH_{zpc} of alumina [39] with hydrolysis of Al ions. However, the presence of organic ligands in WTR leads to less sorption with WTR when compared with alumina.

3.6. FT-IR analysis of WTR

FT-IR spectrum of WTR and dye-loaded WTR is presented in Fig. 7. Bending vibration of hydroxyl group on metal hydroxyl 1,039 cm^{-1} [45,46] which correlates to a weak band of Al–OH. The band near 1,585 cm^{-1} correlated with the C=N and N=N stretching vibrations [47]. The peak near 1,456 cm^{-1} designates vibrations from the symmetrical deformation in esters, stretching and deformation vibration in carbohydrates and aromatic molecules [47]. The peaks in range 2,900 to 2,800 cm^{-1} are related to the stretching vibration C–H bonds [47]. The shifts in the peak at 1,585 cm^{-1} (C=N stretching vibrations) on the surface of WTR to higher numbers with bending vibrations and –OH stretching peaks (3,400–4,000 cm^{-1}) disappeared/absorbed observed after dye adsorption suggest molecular interactions between dye and WTR.

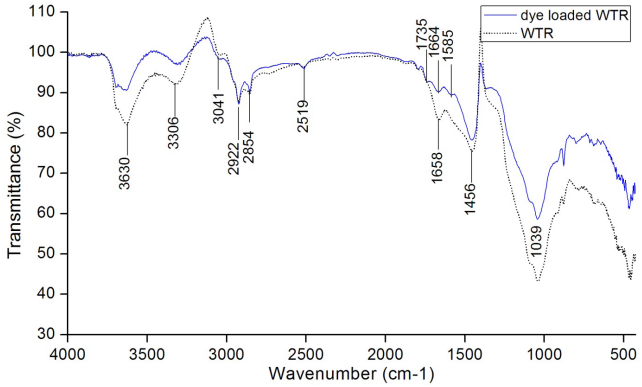

Fig. 7. FT-IR spectrum of WTR before and after sorption.

3.7. Thomas model

Thomas model assumes plug flow behaviour in the bed. Application of Thomas model to the data of C_e/C_o ratios within 5%–95% with respect to bed depths, and flow rate enabled the determination of kinetic coefficients of the system. Analysis of regression coefficients indicated that the regressed lines provided good fit to the experimental data with R^2 values more than 0.8 and adequate fit for values less than 0.8 [48]. Table 4 represents the values of the Thomas model parameters K_{th} and q_m. The experimental (q_{eq}) and predicted (q_m) adsorption capacities at different operational conditions were in close agreement with each other for most of the operating conditions and hence Thomas model can be used for prediction of breakthrough curves.

The capacity of commercially available and modified waste sorbents to uptake disperse dyes from aqueous solution is presented in Table 5. It is important to note that direct comparison of adsorbent capacity of WTR with those reported in the literature is difficult because the experimental conditions applied are different. Table 5 shows that the value of q_m for WTR, 2.90 mg/g, is moderate. However, since WTR is available in large quantities, free of cost, this can be used

Table 4
Parameters of Thomas model under different conditions using linear regression analysis

S. No.	Flow (mL/h)	Bed depth (cm)	q_{eq} (mg/g)	q_m (mg/g)	K_{th} (mL/mg min)	R^2
1	100	5	0.69	0.77	7.43×10^{-2}	0.84
2	100	10	0.95	0.94	7.49×10^{-2}	0.93
3	100	15	0.6	0.35	6.43×10^{-2}	0.93
4	75	10	1.14	1.12	9.85×10^{-3}	0.75
5	75	15	1.00	0.97	9.78×10^{-3}	0.77
6	75	5	1.55	1.54	1.11×10^{-2}	0.72
7	50	5	1.66	1.32	7.80×10^{-3}	0.82
8	50	10	2.90	1.45	1.52×10^{-3}	0.63

Table 5
Comparison of the adsorptive capacity of WTR with other sorbent reported in the literature

S. No.	Adsorbent	Dye	q_m (mg/g)	Reference
1	Bamboo-activated carbon	Disperse Red 167	2.39	[14]
2	Commercial activated carbon (F300)		2.56	
3	Commercial activated carbon (F400)		2.59	
4	Modified cotton fibre	Disperse Yellow 23	7.14	[49]
5	Fly ash	Disperse Red 74	3.89	[50]
6	PPA pre-treated PBO fibre	Disperse Red 60	1.056	[51]
7	Bamboo waste-activated carbon	Disperse Red 167	37.72	[52]
8	Commercial activated carbon (F400)		36.54	
9	Water treatment residuals	Disperse Blue 79	1.84	This study

advantageously. It may be noted that while for most sorbents, regeneration and reuse is generally studied, in the present work this was not attempted since WTR is available in large quantities from water treatment facilities.

3.8. Bed depth service time model

The BDST model is based on physically measuring the capacity of the adsorbent bed at various percentage breakthrough values [53]. The BDST model values can be helpful to scale up the process for other flow rates and influent concentration without further experimental run [54]. The plot of service time against bed height at flow rate of 50, 75 and 100 mL/h is shown in Fig. 8. The model is validated with coefficient of determination value more than 0.8 as presented in Table 6. The storage capacity (S_c) was calculated from the slope assuming linear velocity and constant initial concentration throughout the column operation. The increase in slope with bed height indicates that adsorption of dye is predominated by bed height and flow rate. It is observed that adsorption capacity was higher at low flow rate (50 mL/h) as shown in Table 6. Maximum storage capacity obtained was 702 mg/L at a flow rate of 50 mL/h. The attachment coefficient (K_a) characterises the rate of liquid phase solid transfer onto bed. The larger value of K_a will indicate that even short bed height will take longer to take breakthrough, but as K_a value decreases a progressively larger bed is required to increase the breakthrough time [32]. Moreover, decrease in K_a values with the increase in flow rate indicates that the overall system kinetics was controlled by external mass transfer [54]. Bed depth is considered as the most significant among the different process parameters since with increase in bed depth, contact time of fluid inside column increases, allowing adsorbate molecules to diffuse deeper inside the bed. Thus bed storage capacity (S_c) would change with the service time [32,55].

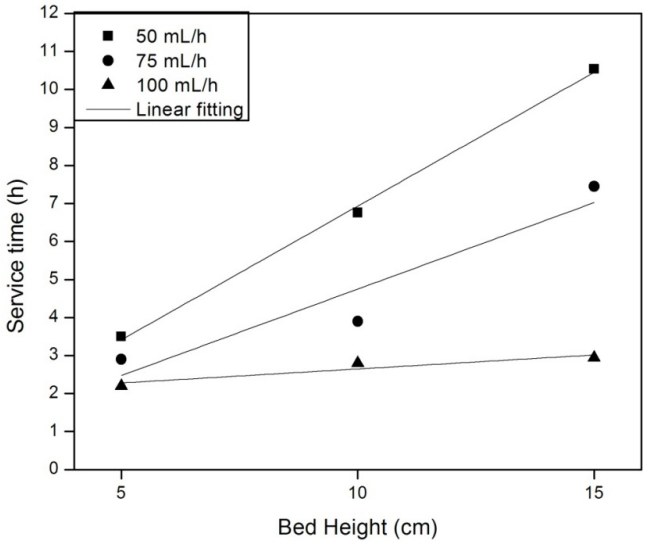

Fig. 8. BDST model plot at 40% breakthrough point.

Table 6
Column data parameters obtained by BDST model at breakthrough point 40%

S. No.	Flow rate (mL/h)	Storage capacity (mg/L)	Attachment coefficient (L/mg h)	R^2
1	50	702	0.21	0.99
2	75	581	0.02	0.82
3	100	149	0.01	0.86

4. Conclusions

The influence of flow rate, contact time and bed depth on the removal of a disperse dye in aqueous solution by WTR was evaluated. The results indicated that the WTR could be used as a low-cost sorbent to remove Disperse Navy Blue 3G. The WTR sorption was analysed using breakthrough curves and it was found that adsorption onto WTR was largely controlled by bed depth and flow rate. The data obtained were successfully modelled using Thomas model. The maximum adsorption capacity of WTR 2.90 mg/g was observed at a flow rate of 50 mL/h. A BDST method was employed to estimate the storage capacity and attachment coefficient for up-scaling of reactor. Present study suggests that though WTR cannot completely remove dye from aqueous solution, this can be used for primary treatment of disperse dye.

References

[1] N.M. Mahmoodi, Photodegradation of dyes using multiwalled carbon nanotube and ferrous ion, J. Environ. Eng., 14 (2013) 1368–1374.
[2] V.K. Gupta, R. Kumar, A. Nayak, T.A. Saleh, M.A. Barakat, Adsorptive removal of dyes from aqueous solution onto carbon nanotubes: a review, Adv. Colloid Interface Sci., 193–194 (2013) 24–34.
[3] A. Salima, B. Benaouda, B. Noureddine, L. Duclaux, Application of *Ulva lactuca* and *Systoceira stricta* algae-based activated carbons to hazardous cationic dyes removal from industrial effluents, Water Res., 47 (2013) 3375–3388.
[4] M.R. Gadekar, M.M. Ahammed, Coagulation/flocculation process for dye removal using water treatment residuals: modelling through artificial neural networks, Desal. Wat. Treat., 57 (2016) 26392–26400.
[5] T. Ngulube, J.R. Gumbo, V. Masindi, A. Maity, An update on synthetic dyes adsorption onto clay based minerals: a state-of-art review, J. Environ. Manage., 191 (2017) 35–57.
[6] M. Vakili, M. Rafatullah, B. Salamatinia, A. Zuhairi, M. Hakimi, K. Bing, Z. Gholami, P. Amouzgar, Application of chitosan and its derivatives as adsorbents for dye removal from water and wastewater: a review, Carbohydr. Polym., 113 (2014) 115–130.
[7] C.S. Oliveira, C. Airoldi, Pyridine derivative covalently bonded on chitosan pendant chains for textile dye removal, Carbohydr. Polym., 102 (2014) 38–46.
[8] T.A. Nguyen, R.S. Juang, Treatment of waters and wastewaters containing sulfur dyes: a review, Chem. Eng. J., 219 (2013) 109–117.
[9] H. Karimi, M. Ghaedi, Application of artificial neural network and genetic algorithm to modeling and optimization of removal of methylene blue using activated carbon, J. Ind. Eng. Chem., 20 (2014) 2471–2476.
[10] M.A.M. Salleh, D.K. Mahmoud, W.A.W.A. Karim, A. Idris, Cationic and anionic dye adsorption by agricultural solid wastes: a comprehensive review, Desalination, 280 (2011) 1–13.
[11] S.-S. Mehdi, A. Khataee, S.W. Joo, Kinetics and equilibrium studies of removal of an azo dye from aqueous solution by adsorption onto scallop, J. Ind. Eng. Chem., 20 (2014) 610–615.

[12] C.R. Holkar, A.J. Jadhav, D.V. Pinjari, N.M. Mahamuni, A.B. Pandit, A critical review on textile wastewater treatments: possible approaches, J. Environ. Manage., 182 (2016) 351–366.
[13] S. Xu, J. Chen, B. Wang, Y. Yang, Molecular surface area based predictive models for the adsorption and diffusion of disperse dyes in polylactic acid matrix, J. Colloid Interface Sci., 458 (2015) 22–31.
[14] L. Wang, Application of activated carbon derived from "waste" bamboo culms for the adsorption of azo disperse dye: kinetic, equilibrium and thermodynamic studies, J. Environ. Manage., 102 (2012) 79–87.
[15] S. Nethaji, A. Sivasamy, R.V. Kumar, A.B. Mandal, Preparation of char from lotus seed biomass and the exploration of its dye removal capacity through batch and column adsorption studies, Environ. Sci. Pollut. Res., 20 (2013) 3670–3678.
[16] T. Ahmad, K. Ahmad, A. Ahad, M. Alam, Characterization of water treatment sludge and its reuse as coagulant, J. Environ. Manage., 182 (2016) 606–611.
[17] A.T. Nair, M.M. Ahammed, Coagulant recovery from water treatment plant sludge and reuse in post-treatment of UASB reactor effluent treating municipal wastewater, Environ. Sci. Pollut. Res., 21 (2014) 10407–10418.
[18] T. Ahmad, K. Ahmad, M. Alam, Sustainable management of water treatment sludge through 3'R' concept, J. Cleaner Prod., 124 (2016) 1–13.
[19] J. Jiao, J. Zhao, Y. Pei, Adsorption of Co(II) from aqueous solutions by water treatment residuals, J. Environ. Sci. (China), 52 (2016) 232–239.
[20] W. Chu, Dye removal from textile dye wastewater using recycled alum sludge, Water Res., 35 (2001) 3147–3152.
[21] A.O. Babatunde, Y.Q. Zhao, Constructive approaches toward water treatment works sludge management: an international review of beneficial reuses, Crit. Rev. Environ. Sci. Technol., 37 (2007) 129–164.
[22] P. Prakash, A.K. Sengupta, Selective coagulant recovery from water treatment plant residuals using donnan membrane process, Environ. Sci. Technol., 37 (2003) 4468–4474.
[23] N. Muisa, Z. Hoko, P. Chifamba, Impacts of alum residues from Morton Jaffray Water Works on water quality and fish, Harare, Zimbabwe, Phys. Chem. Earth, 36 (2011) 853–864.
[24] S.S. Moghaddam, A.R.M. Moghaddam, M. Arami, Response surface optimization of acid red 119 dye from simulated wastewater using Al based waterworks sludge and polyaluminium chloride as coagulant, J. Environ. Manage., 92 (2011) 1284–1291.
[25] S.S. Moghaddam, A.M.R. Moghaddam, M. Arami, Coagulation/flocculation process for dye removal using sludge from water treatment plant: optimization through response surface methodology, J. Hazard. Mater., 175 (2010) 651–657.
[26] K. Jung, M. Hwang, D. Park, K. Ahn, Comprehensive reuse of drinking water treatment residuals in coagulation and adsorption processes, J. Environ. Manage., 181 (2016) 425–434.
[27] K.C. Makris, D. Sarkar, R. Datta, Aluminum-based drinking-water treatment residuals: a novel sorbent for perchlorate removal, Environ. Pollut., 140 (2006) 9–12.
[28] W. Wang, C. Ma, Y. Zhang, S. Yang, Y. Shao, X. Wang, Phosphate adsorption performance of a novel filter substrate made from drinking water treatment residuals, J. Environ. Sci., 45 (2016) 191–199.
[29] K.D. Quiñones, A. Hovsepyan, A. Oppong-Anane, J.C.J. Bonzongo, Insights into the mechanisms of mercury sorption onto aluminum based drinking water treatment residuals, J. Hazard. Mater., 307 (2016) 184–192.
[30] Y. Wai, K. Ghyselbrecht, R.M. Santos, J.A. Martens, R. Swennen, V. Cappuyns, B. Meesschaert, Adsorption of multi-heavy metals onto water treatment residuals: sorption capacities and applications, Chem. Eng. J., 200–202 (2012) 405–415.
[31] H. Soleimanifar, Y. Deng, L. Wu, D. Sarkar, Water treatment residual (WTR)-coated wood mulch for alleviation of toxic metals and phosphorus from polluted urban stormwater runoff, Chemosphere, 154 (2016) 289–292.
[32] M.T. Uddin, M. Rukanuzzaman, M.M. Khan, M.A. Islam, Adsorption of methylene blue from aqueous solution by jackfruit (*Artocarpus heterophyllus*) leaf powder: a fixed-bed column study, J. Environ. Manage., 90 (2009) 3443–3450.
[33] USEPA, Test Method 3050B: Acid Digestion of Sediments, Sludges, and Soils, Hazard. Waste Test Methods/SW-846, USEPA, 1996, pp. 1–12.
[34] A.A. Ahmad, B.H. Hameed, Fixed-bed adsorption of reactive azo dye onto granular activated carbon prepared from waste, J. Hazard. Mater., 175 (2010) 298–303.
[35] R. Han, Y. Wang, W. Zou, Y. Wang, J. Shi, Comparison of linear and nonlinear analysis in estimating the Thomas model parameters for methylene blue adsorption onto natural zeolite in fixed-bed column, J. Hazard. Mater., 145 (2007) 331–335.
[36] S. Chen, Q. Yue, B. Gao, Q. Li, X. Xu, K. Fu, Adsorption of hexavalent chromium from aqueous solution by modified corn stalk: a fixed-bed column study, Bioresour. Technol., 113 (2012) 114–120.
[37] A.M. Saatci, C.S. Oulman, The bed depth service time design method for deep bed filtration, J. Am. Water Works Assoc., 72 (1980) 524–528.
[38] Y. Zhang, Y. Jia, Fluoride adsorption onto amorphous aluminum hydroxide: roles of the surface acetate anions, J. Colloid Interface Sci., 483 (2016) 295–306.
[39] S. Goldberg, J.A. Davis, J.D. Hem, The Environmental Chemistry of Aluminum, 2nd Ed., CRC Publishers, 1996.
[40] Z. Alimohammadi, H. Younesi, N. Bahramifar, Batch and column adsorption of reactive red 198 from textile industry effluent by microporous activated carbon developed from walnut shells, Waste Biomass Valorization, 7 (2016) 1255–1270.
[41] A. Hethnawi, N.N. Nassar, A.D. Manasrah, G. Vitale, Polyethylenimine-functionalized pyroxene nanoparticles embedded on diatomite for adsorptive removal of dye from textile wastewater in a fixed-bed column, Chem. Eng. J., 320 (2017) 389–404.
[42] T. Zhou, W. Lu, L. Liu, H. Zhu, Y. Jiao, S. Zhang, R. Han, Effective adsorption of light green anionic dye from solution by CPB modified peanut in column mode, J. Mol. Liq., 211 (2015) 909–914.
[43] C.H. Giles, T.H. MacEwan, S.N. Nakhwa, D. Smith, Studies in adsorption. Part XI.* A system of classi$cation of solution adsorption isotherms, and its use in diagnosis of adsorption mechanisms and in measurement of specific surface areas of solids, J. Chem. Soc., 0 (1960) 3973–3993.
[44] P. Liu, Y. Li, Q. Wen, C. Dong, G. Pan, Mechanism and kinetics of aluminum dissolution during copper sorption by acidity paddy soil in South China, J. Environ. Sci., 34 (2015) 100–106.
[45] Y. Zhang, M. Yang, X.-M. Dou, H. He, D.-S. Wang, Arsenate adsorption on an Fe-Ce bimetal oxide adsorbent: role of surface properties, Environ. Sci. Technol., 39 (2005) 7246–7253.
[46] S. Sadaf, H.N. Bhatti, S. Alia, K. Rehman, Removal of Indosol Turquoise FBL dye from aqueous solution by bagasse, a low cost agricultural waste: batch and column study, Desal. Wat. Treat., 52 (2014) 184–198.
[47] T. Yadav, A.A. Mungray, A.K. Mungray, Effect of TiO_2 nanoparticles on UASB biomass activity and dewatered sludge, Environ. Technol., 38 (2017) 413–423.
[48] R. Han, D. Ding, Y. Xu, W. Zou, Y. Wang, Y. Li, L. Zou, Use of rice husk for the adsorption of congo red from aqueous solution in column mode, Bioresour. Technol., 99 (2008) 2938–2946.
[49] Y. Mao, Y. Guan, Q.K. Zheng, X.N. Feng, X.X. Wang, Adsorption thermodynamic and kinetic of disperse dye on cotton fiber modified with tolylene diisocyanate derivative, Cellulose, 18 (2011) 271–279.
[50] D. Sun, X. Zhang, Y. Wu, T. Liu, Kinetic mechanism of competitive adsorption of disperse dye and anionic dye on fly ash, Int. J. Environ. Sci. Technol., 10 (2013) 799–808.
[51] Y. Guan, Y. Mao, D. Wei, X. Wang, P. Zhu, Adsorption thermodynamics and kinetics of disperse dye on poly (p-phenylene benzobisoxazole) fiber pretreated with polyphosphoric acid, Korean J. Chem. Eng., 30 (2013) 1810–1818.
[52] L. Wang, Removal of Disperse Red dye by bamboo-based activated carbon: optimisation, kinetics and equilibrium, Environ. Sci. Pollut. Res., 20 (2013) 4635–4646.

[53] S. Sadaf, H.N. Bhatti, Evaluation of peanut husk as a novel, low cost biosorbent for the removal of Indosol Orange RSN dye from aqueous solutions: batch and fixed bed studies, Clean Technol. Environ. Policy, 16 (2014) 527–544.
[54] K.S. Bharathi, S.P.T. Ramesh, Fixed-bed column studies on biosorption of crystal violet from aqueous solution by *Citrullus lanatus rind* and *Cyperus rotundus*, Appl. Water Sci., 3 (2013) 673–687.
[55] R. Han, Y. Wang, X. Zhao, Y. Wang, F. Xie, J. Cheng, M. Tang, Adsorption of methylene blue by phoenix tree leaf powder in a fixed-bed column: experiments and prediction of breakthrough curves fixed-bed column: experiments and prediction, Desalination, 245 (2009) 284–297.